Proceedings of
International Conference on
Fluid Engineering
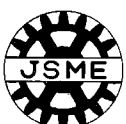
VOL. III

ICFE '97

July 13 - 16, 1997

Tokyo International Forum, Tokyo, Japan

Organized by   Fluid Engineering Division, JSME

Co-organized by   Fluids Engineering Division, ASME

                      Thermal and Fluids Engineering Division, KSME

The Fluid Engineering Division
THE JAPAN SOCIETY OF MECHANICAL ENGINEERS

JSME CENTENNIAL GRAND CONGRESS
Tokyo, Japan : July 13 - August 3, 1997

General Chair : Yujiro HAYASHI, Kanazawa University

(Grand Congress Executive Committee)

Yuji FURUKAWA, Tokyo Metropolitan University
Shigeo HIROSE, Tokyo Institute of Technology
Isao SATOH, Tokyo Institute of Technology
Kohei SUZUKI, Tokyo Metropolitan University

Fumio HARA, Science University of Tokyo
Shigefumi NISHIO, The University of Tokyo
Toshiyuki SAWA, Yamanashi University
Gen YAMADA, Hokkaido University

(Grand Congress Organizing Committee)

Yasuhiro DAISHO, Waseda University
Yasunobu FUJITA, Kyushu University
Fumio HARA, Science University of Tokyo
Manabu KIUTI, The University of Tokyo
Akira MATSUMOTO, Ministry of Transport
Yoichiro MATSUMOTO, The University of Tokyo
Shuzo MIWA, Aoyama Gakuin University
Juhachi ODA, Kanazawa University
Hideo OHASHI, Kogakuin University
Yoshiaki OOKAMI, Tokyo Institute of Technology
Katsuhiko SHIMIZU, Ebara Corporation
Kazuo TANISHITA, Keio University
Ryuhei YAMAGUCHI, Shibaura Institute of Technology
Kazuo YOSHIDA, Keio University

Masakatsu FUJIE, Hitachi, Ltd.
Hiroaki FUNAHASHI, Tokyo Institute of Technology
Yoshimi ITO, Tokyo Institute of Technology
Aizo KUBO, Kyoto University
Shiro MATSUMOTO, Saitama University
Fumio MATSUOKA, Mitsubishi Electric Corporation
Akira NAGASHIMA, Keio University
Keiji OGURA, Osaka Technology
Kyosuke ONO, Tokyo Institute of Technology
Masamichi SHIGEHARA, Tokyo Metropolitan Inst. Tech.
Satoshi SOUMIYA, Keio University
Kazuo YAMAFUJI, University of Electro-Communications
Hiroshi YAMAKAWA, Waseda University
Haruo YOSHIKI, The University of Tokyo

Rotordynamic Forces from Discharge-to-Suction Leakage Flows in Centrifugal Pumps : Effects of Geometry

Robert V. Uy, Brian L. Bircumshaw
and Christopher E. Brennen
Department of Mechanical Engineering
California Institute of Technology
Pasadena, California

ABSTRACT

The rotordynamic forces generated by the fluid flow through the impeller leakage path of a centrifugal pump are now well established. The present paper examines the effects of modifying the leakage path geometry by changing the front shroud, from a conical shape to a more typical curved design, and the effects of low pressure seal design on these forces. It is found that only the cross-coupled stiffness is affected by the change of path geometry. Changing the low pressure seal from an axial to a radial clearance does, however, significantly affect the rotordynamic forces. A bulk flow numerical model is found to predict the same general result for the low pressure seal tests. The model agrees with the general trends with increasing leakage flow coefficient exhibited by the data, but appears to underpredict the magnitude of the normal force.

INTRODUCTION

Previous experimental and analytical results have shown that discharge-to-suction leakage flows in shrouded centrifugal pumps contribute substantially to the fluid-induced rotordynamic forces (1). Experiments conducted in the Rotor Force Test Facility (RFTF) at Caltech on an impeller undergoing a predetermined whirl have shown that the leakage flow contributions to the normal and tangential forces can be as much as 70% and 30% of the total, respectively (9). Other experiments have examined the consequences of leakage flows and have shown that the rotordynamic forces are functions not only of whirl ratio, but also of the leakage flow rate and the impeller shroud to pump housing clearance. The forces were found to be inversely proportional to the clearance. A region of forward subsynchronous whirl was found for which the average tangential force was destabilizing. This region decreased with increasing flow coefficient (7).

The present paper compares a contoured shroud and casing, which is more typical of leakage path geometries, with the conical shroud and casing used previously by Guinzburg (5,6,7) and Sivo (10,11). We also explore the effect of having an axial versus radial clearance low pressure seal at the leakage path discharge. Experimental results are compared with the predictions of a modified version of Childs' (4) bulk flow model.

ROTORDYNAMIC FORCES

Figure (1) shows a schematic of the hydrodynamic forces that act on a rotating impeller whirling in a circular orbit. The unsteady fluid forces acting on the impeller due to the imposed whirl motion (eccentricity ϵ, whirl frequency Ω) are decomposed into a force normal to the direction of whirl motion, F_n, and a force in the direction of forward whirl motion, F_t (9). The normal and tangential forces are traditionally presented in dimensionless form as functions of the whirl frequency ratio, Ω/ω. More specifically, it is convenient for rotordynamicists to fit F_n, to a quadratic function of the whirl frequency ratio, Ω/ω, and to fit the dimensionless tangential force, F_t, to a linear function. The resulting expressions are given by:

$$F_n = M \left(\frac{\Omega}{\omega}\right)^2 - c \left(\frac{\Omega}{\omega}\right) - K \qquad (1)$$

$$F_t = -C \left(\frac{\Omega}{\omega}\right) + k \qquad (2)$$

where the dimensionless coefficients are the direct added mass (M), direct damping (C), cross-coupled damping (c), direct stiffness (K), and the cross-coupled stiffness (k). As can be seen from equation (2), a positive cross-coupled stiffness is destabilizing because it promotes whirl motion of the impeller for a range of

positive subsynchronous frequencies. It is also the tangential force acting at zero whirl ratio. From equation (1), a large negative direct stiffness is also destabilizing since it promotes a positive normal force which would tend to increase the eccentricity of the whirl orbit.
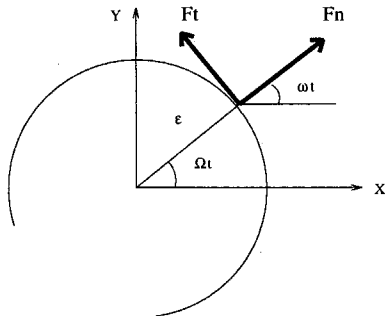

FIGURE 1: Schematic of the fluid-induced forces acting on an impeller whirling in a circular orbit.

A convenient measure of the rotordynamic stability is the ratio of cross-coupled stiffness to the direct damping (i.e. k/C) which is termed the whirl ratio. This defines the range of positive whirl frequency ratios for which the tangential force is destablizing.

TEST APPARATUS

The present experiments were conducted in the Rotor Force Test Facility (RFTF) at Caltech (9). The working fluid is water. The main components of the test section apparatus consist of a solid or dummy impeller (the rotating shroud), a housing (the stationary shroud), the rotating dynamometer (or internal force balance), an eccentric whirl mechanism, and a leakage discharge seal with either axial or radial clearance. The test section, with the conical rotor and stator forming the leakage path, is shown in Figure (2). The contoured rotor and stator form the leakage path depicted in Figure (3). For illustration purposes, Figure (2) shows a low pressure seal with axial clearance and Figure (3) shows a seal with radial clearance. The purpose of this type of experimental test is to isolate the leakage flow forces by using a solid impeller.

The geometry of the contoured rotor and stator differ from that of the conical rotor and stator previously used and described by Guinzburg (5,6,7) and Sivo (10,11). The contoured rotor was designed with a 3rd order curve fit such that the contour was parallel to the centerline at the eye and perpendicular to the centerline at the tip. A matching stator was constructed to maintain a constant normal clearance $H = 0.30cm$. This geometry was chosen to more closely model a typical centrifugal pump impeller shroud.
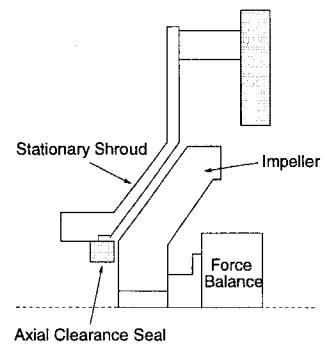

FIGURE 2: Experimental Setup, Conic Shroud.

The rotor is mounted directly on the rotating dynamometer which in turn is connected to a data acquisition system which permits measurements of the rotor-dynamic force matrix components (9). The eccentric drive mechanism imposes a circular whirl orbit on the basic main shaft rotation. The radius of the whirl orbit (eccentricity) can be varied but the present experiments used one eccentricity $\epsilon = 0.025cm$, since previous experiments clearly demonstrated that this lay within the linear response regime. The low pressure seal at the leakage exit models a wear ring or an annular seal. Flow through the leakage path is generated by an auxiliary pump.
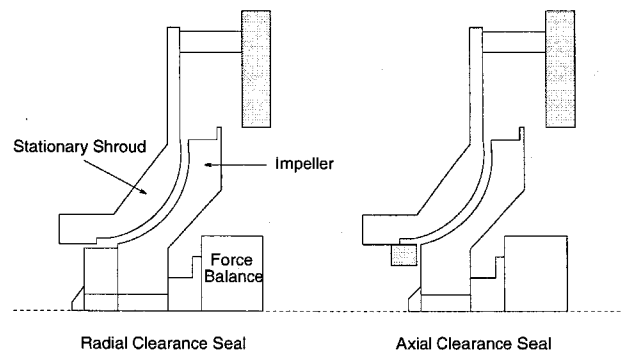

FIGURE 3: Experimental Configuration: Contoured Shroud with radial clearance (left) and axial clearance (right) low pressure seal.

In addition to comparing the results for the contoured and conical leakage path geometries, the present investigation also examined the effects of different types of seals at the low pressure end of the leakage path. Both an axial clearance seal and a radial clearance seal were tested. The low pressure axial clearance seal models a face seal. The distance from the outer radius of the impeller eye to the inner radius of the seal was $1.14cm$.

The axial clearance was set to $0.05cm$. The low pressure radial clearance seal models a turbulent annular seal. The geometry was selected to match the leakage path volume (between the seal surface and the impeller) of the axial clearance seal. To do so, a sealing section of axial length $0.51cm$ was formed between the rotating member and the stator and an imposed radial clearance of $0.09cm$ was used to accomodate the eccentricity.

BULK FLOW MODEL

A bulk flow model of the discharge-to-inlet leakage flow was developed by Childs (4)(and used by Guinzburg (5)). This model is employed, (with some modifications) in the present paper to compare with the experimental results.

The bulk flow model predicted large resonances in the calculated forces for cases in which inlet swirl was present. It was observed that these resonances could be substantially reduced if, in Childs' (4) analysis, the β_0 and β_1 factors of the path velocity term $A_{3\theta}$ in the first-order circumferential momentum equation were set to zero. This corresponds to a case in which the product of the eccentricity and the first- order path velocity is small compared to the zero-order path velocity in the wall shear terms. While this approximation is arbitrary (but plausible), it is clear that it plays a very significant role in the prediction of the forces. One practical advantage is that it allows comparison of the general trends predicted by the model without the confusion the resonances introduce.

The frictional shear stresses in the model were based on the work of Yamada (12) and are defined by:

$$\frac{\tau}{\frac{1}{2}\rho u^2} = n \left(\frac{\rho u h}{\eta} \right)^m \qquad (3)$$

where u is the relative velocity between the average or bulk flow in the annulus and the solid surface and coefficients, m and n, can be different for the shear stress on the stator (ms and ns) and on the rotor (mr and nr). These are based originally on the work of Hirs (8) who does, however, recommend that the coefficients m and n be "fitted to individual experiments." The frictional coefficients are dependent on various physical parameters, including the curvature of the surface, inertial effects, and roughness.

In the present calculations, the frictional exponents $ms = $ -0.25 and $mr = $ -0.25 were retained as they correspond to the fully turbulent flow which occurs in the annulus. The frictional factors of $ns = .13$ and $nr = .08$ were used as they generated roughly similar trends to the experimental data. A constant impeller speed, ω, of 1000 rpm was used and forces calculated over a range of whirl frequency ratios, $-0.7 < \Omega/\omega < 0.7$.
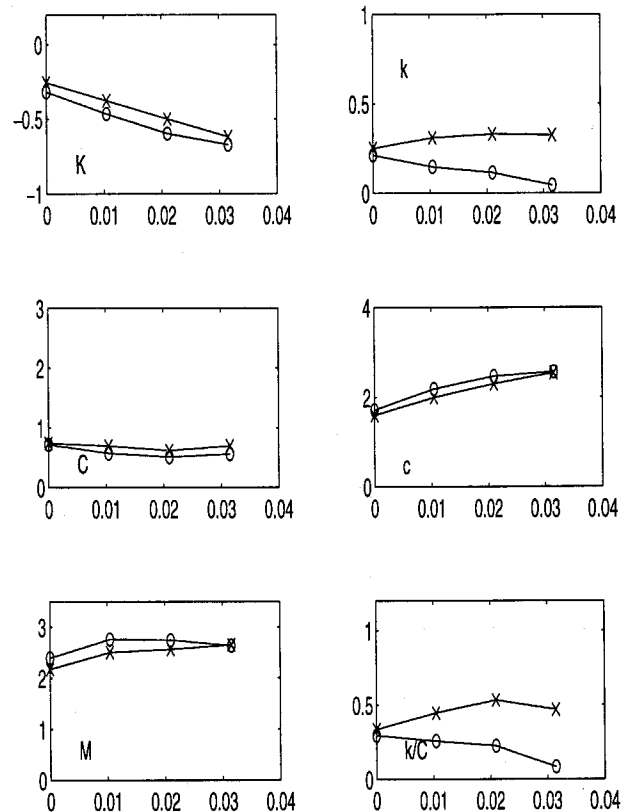

FIGURE 4: Rotordynamic force coefficients as functions of the flow coefficient ϕ for experimental tests with the conical (o) and contoured shroud (x).

EXPERIMENTAL RESULTS

For this analysis, a constant impeller speed, ω, of 1000 rpm was used. The rotordynamic force coefficients were derived from a least squares quadratic and linear fit of the normal and tangetial forces respectively. F_n and F_t were measured over the range of whirl frequency ratios, $-0.7 < \Omega/\omega < 0.7$. Figure (4) presents the dimensionless rotordynamic force coefficients as functions of the leakage flow coefficient, and compares the conical and contoured leakage path geometries. Except for the cross-coupled stiffness, all of the rotordynamic force coefficients match in both trend and magnitude, showing that the effect of the geometry of the passage (as opposed to the clearance) is relatively small. The coefficients K, c, M, are virtually identical, reflecting the fact that the geometry has little effect on the normal force, F_n. The tangential force, F_t, is uniformly shifted over the entire whirl frequency range, producing the shift in cross-coupled stiffness, k. However, the shift only develops as the flow rate increases. The reason for this is

not currently understood.

The change in k produces a corresponding change in the whirl ratio, k/C. Earlier, both Guinzburg (7) and Sivo (11) reported that, with the conical geometry, the whirl ratio decreased with increasing flow coefficient, and this is confirmed with the present experiments with the conical geometry. However, the contoured geometry produces a k/C which increases with increasing flow coefficient.

Figure (5) presents the dimensionless rotordynamic force coefficients obtained from the low pressure seal experiments as functions of the leakage flow coefficient. For the radial clearance seal, the cross-coupled stiffness and direct damping increase with increasing flow coefficient while for the axial clearance seal, the coefficients of the tangential force remain relatively constant. It is evident that the geometry of the seal as well as the flow rate can have substantial effects on the rotordynamic coefficients. We will comment below on the differences in the contributions which the two seals make to the rotordynamic coefficients.

BULK FLOW ANALYSIS RESULTS

The rotordynamic force coefficients obtained from the bulk flow model for both seal configurations are presented in Figure (6). Using the frictional coefficients mentioned previously, the results show qualitative agreement with the experimental data, but also some substantial discrepancies. The cross-coupled stiffness and direct damping appear to be slightly underpredicted in comparison to the experiments, but the same trends with flow coefficient are observed in both seal configurations. The cross-coupled damping, c, matches the experimental results fairly closely for both seals. The direct-added mass term M is underpredicted by the model. The direct stiffness, K, is poorly predicted in both configurations.

We conclude that though the bulk flow model seems to be roughly correct in predicting some of the rotordynamic coefficients, there are some characteristics (such as the direct stiffness) in which the comparison with the experiments are unsatisfactory. There are, however, uncertainties in the model (such as the frictional coefficients and the boundary conditions) which require further exploration and such a project could lead to important improvements in the bulk flow model.

CONCLUSIONS

The influence of leakage path geometry on the rotordynamic forces in shrouded centrifugal pumps has been examined. A comparison between a straight leakage path formed by a conical rotor and stator, and a curved leakage path formed by a contoured rotor and stator, revealed that only the tangential force and cross-coupled stiffness were substantially affected. Other

than this, the geometry of the leakage path (as opposed to the clearance) appears to have little effect upon the rotordyanmic coefficients.

The influence of the low pressure seal design on the rotordynamic forces in a typical shrouded centrifugal pump was investigated, and here large differences were observed in the results for an axial clearance and a radial clearance seal. It is evident that, apart from its effect upon the flow rate, the geometry of the seal can have substantial effects on the rotordynamic coefficients, and, in particular, on the direct and cross-coupled stiffness, K and k, and on the direct damping C. The effects on the cross-coupled damping, c, and the direct added mass, M, were less significant. Moreover, the variations of K, k and C with flow rate are quite different for the two seals. For example, with the radial clearance seal, the direct stiffness, K, increased dramatically with flow rate. This may be simply the Lomakin effect (3) contribution from the radial clearance seal. The radial clearance seal also leads to larger tangential forces, though the effect on the whirl ratio, k/C is small since both k and C seem to increase by equal amounts.

Finally, this paper has also presented comparisons of the experimental rotordynamic coefficients with those predicted by a modified version of Childs' bulk flow model. While the model seems to predict some of the rotordynamic characteristics reasonably well, there are other coefficients and trends which are not at all well predicted. Perhaps further improvements in the model (for example, improved understanding of the frictional coefficients or boundary conditions) could lead to a more accurate predictive and design tool.

ACKNOWLEDGEMENTS

NOMENCLATURE

$[A^*]$	Rotordynamic force matrix
C	Direct damping coefficient, normalized by $\rho\pi\omega^2 R_2^2 L\varepsilon$
c	Cross-coupled damping coefficient, normalized by $\rho\pi\omega^2 R_2^2 L\varepsilon$
F_n	Force normal to whirl orbit normalized by $\rho\pi\omega^2 R_2^2 L\varepsilon$
F_t	Force tangent to whirl orbit normalized by $\rho\pi\omega^2 R_2^2 L\varepsilon$
H	Clearance between impeller shroud and housing
h	Film thickness
K	Direct stiffness coefficient,

	normalized by $\rho\pi\omega^2 R_2^2 L\varepsilon$
k	Cross-coupled stiffness coefficient, normalized by $\rho\pi\omega^2 R_2^2 L\varepsilon$
L	Axial length of the impeller
M	Direct added mass coefficient, normalized by $\rho\pi\omega^2 R_2^2 L\varepsilon$
mr, ms	Empirical exponent for rotor and stator respectively
nr, ns	Empirical constants for rotor and stator respectively
R_2	Radius of impeller and leakage inlet
u_s	Mean leakage inlet path velocity of fluid
η	Dynamic viscosity
ε	Eccentricity of whirl orbit
ρ	Fluid density
ϕ	Leakage flow coefficient, $u_s/\omega R_2$
ω	Main shaft radian frequency
Ω	Whirl radian frequency
τ	Wall shear stress

REFERENCES

1. Adkins, D. and Brennen, C.E., 1988, Analysis of Hydrodynamic Radial Forces on Centrifugal Pump Impellers, ASME *Journal of Fluids Engineering*, Vol. 110, No. 1, pp. 20-28.

2. Baskharone, E., and Hensel, S., 1993, Flow Field in the Secondary, Seal-Containing Passages of Centrifugal Pumps, ASME *Journal of Fluids Engineering*, Vol. 115, pp. 702-709.

3. Brennen, C.E., 1994. Hydrodynamics of Pumps, Concepts ETI and Oxford University Press.

4. Childs, D.W., 1989, Fluid-Structure Interation Forces at Pump-Impeller-Shroud Surfaces for Rotordynamic Calculations, ASME *Journal of Vibrations, Acoustics, Stress, and Reliablity in Design*, Vol. 111, pp. 216-225.

5. Guinzburg, A., 1992, Rotordynamic Forces Generated By Discharge-to-Suction Leakage Flows in Centrifugal Pumps, Ph.D. Thesis, California Institute of Technology.

6. Guinzburg, A., Brennen, C.E., Acosta, A.J., and Caughey, T.K., 1993, The Effect of Inlet Swirl on the Rotordynamic Shroud Forces in a Centrifugal Pump, ASME *Journal of Engineering for Gas Turbines and Power*, Vol. 115, No. 2, pp. 287-293.

7. Guinzburg, A., Brennen, C.E., Acosta, A.J., and Caughey, T.K., 1994, Experimental Results for the Rotordynamic Characteristics of Leakage Flows in Centrifugal Pumps, ASME *Journal of Fluids Engineering*, Vol. 116, No. 1, pp. 110-115.

8. Hirs, G., 1973, A Bulk-Flow Theory For Turbulence in Lubricant Films, ASME *Journal of Lubrication Technology*, April, pp.137-146.

9. Jery, B., 1986, Experimental Study of Unsteady Hydrodynamic Force Matrices on Whirling Centrifugal Pump Impellers, Ph.D. Thesis, California Institute of Technology.

10. Sivo, J., Acosta, A.J., Brennen, C.E., Caughey, T.K., Ferguson, T., and Lee, G., 1994, Laser Velocimeter Measurements in the Leakage Annulus of a Whirling Centrifugal Pump, ASME *Laser Anemometry-1994, Advances and Applications* FED-Vol. 191, pp. 111-117.

11. Sivo, J., Acosta, A.J., Brennen, C.E., and Caughey, T.K., 1995, The Influence of Swirl Brakes on the Rotordynamic Forces Generated by Discharge-to-Suction Leakage Flows in Centrifugal Pumps, ASME *Journal of Fluids Engineering*, Vol. 117, No. 1, pp. 104-108.

12. Yamada, Y., 1962, Resistance of Flow Through an Annulus with an Inner Rotating Cylinder, *Bulletin of JSME*, Vol. 5, pp. 302-310.
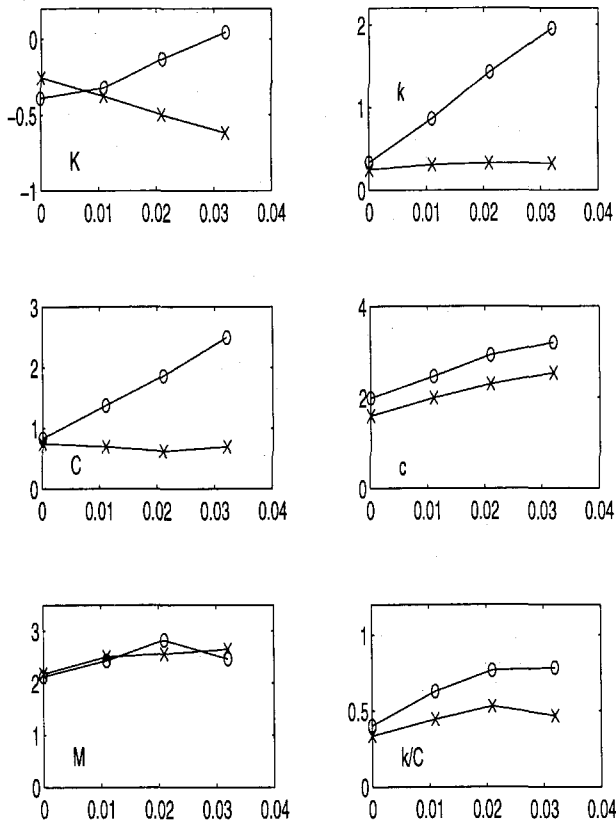
FIGURE 5: Rotordynamic force coefficients as functions of the flow coefficient ϕ for the experiments with low pressure seals having an axial clearance (x), and a radial clearance (o).
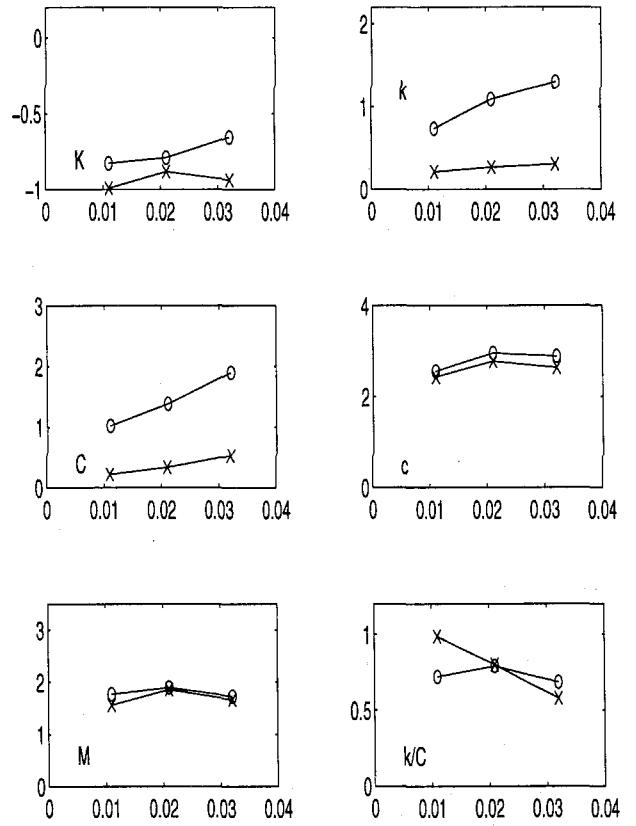
FIGURE 6: Rotordynamic force coefficients as functions of the flow coefficient, ϕ, for Childs' model for low pressure seals having an axial clearance (x), and a radial clearance (o).